IMPLEMENTATION AND PERFORMANCE RESULTS FOR TRELLIS DETECTION OF SOQPSK

Mark Geoghegan
Nova Engineering Inc., Cincinnati, OH

ABSTRACT

Shaped Offset QPSK (SOQPSK), as proposed and analyzed by Terrance Hill, is a family of constant envelope waveforms that is non-proprietary and exhibits excellent spectral containment and detection efficiency. Results using a conventional coherent OQPSK demodulator without any special pulse shaping to recover the SOQPSK signal have been previously presented. This paper describes a trellis detector for SOQPSK-A and SOQPSK-B that provides superior detection performance, as compared to a traditional OQPSK detector, by accounting for the pulse shaping. Analytical error performance bounds, implementation of the trellis demodulator, and computer simulation results are presented.

KEY WORDS

SOQPSK, Trellis Detection, Spectral Efficiency, Power Efficiency.

INTRODUCTION

SOQPSK is a non-proprietary modulation technique that is quickly gaining popularity in both terrestrial and space applications. The family of SOQPSK waveforms, as described by Hill [1], are constant envelope signals with excellent spectral containment and detection efficiency. Furthermore, they can be detected using a standard OQPSK receiver. Performance results from Hill [1] and Younes, Brase, Patel, and Wesdock [2] indicate that a penalty of 2 dB or more are incurred with SOQPSK-A and SOQPSK-B respectively, if a suboptimum OQPSK detector is used. The objective of this paper is to investigate the optimum receivers for these waveforms, characterize their performance, and provide a framework for designing a high-speed implementation of the processing algorithms. This paper is composed of five sections that include a brief review of SOQPSK, analysis of the attainable detection performance, implementation, simulation results, and the conclusion.

DESCRIPTION OF SOQPSK

The SOQPSK waveforms described by Hill [1] are constant envelope, continuous phase modulations that allow a designer to easily trade-off spectral and power efficiency by varying a few simple parameters. The waveforms are completely described by either their instantaneous phase or frequency. Figure 1 illustrates a conceptual SOQPSK modulator that maps a binary input stream a(i) into ternary-valued (+1, 0, -1) frequency impulses $\alpha(t)$, passes them through a shaping filter with response g(t), and applies the instantaneous frequency f(t) or phase $\phi(t)$ to an appropriate modulator which produces the desired SOQPSK waveform.

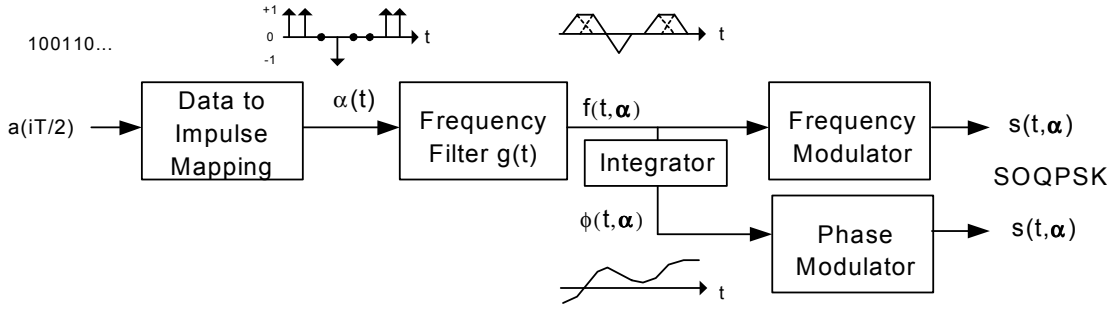

Figure 1. SOQPSK Modulator

The frequency pulse shapes for SOQPSK are given by g(t) = n(t) * w(t), where

$$n(t) = \frac{A\cos(\pi\rho Bt/T)}{1-4(\rho Bt/T)^2} * \frac{\sin(\pi Bt/T)}{(\pi Bt/T)}\ ,\ w(t) = \begin{cases} 1, & for\ \ |t/T| < T \\ \frac{1}{2} + \frac{1}{2}\cos\frac{\pi(|t/T| - T_1)}{T_2}, & for\ \ T_1 < |t/T| < T_1 + T_2 \\ 0, & for\ \ |t/T| > T_1 + T_2 \end{cases}$$

Note that the four parameters ρ, B, T_1, and T_2 serve to completely define the frequency pulse shapes for SOQPSK-A and SOQPSK-B, as well as an infinite set of similar, and interoperable, waveforms. The specific values for SOQPSK-A and SOQPSK-B are listed in Table 1 and the resulting pulse shapes and spectra are plotted in Figures 2 and 3. For comparison purposes, the spectrum of the MIL-STD-188-182 SOQPSK, which uses a rectangular frequency pulse, is also included. The dramatic reduction in sidelobe energy makes SOQPSK-A and SOQPSK-B very attractive for terrestrial, satcom, and space applications. Moreover, these waveforms can be recovered with a conventional OQPSK demodulator if a moderate penalty in detection efficiency can be tolerated. Simulation results from [1] and [2] indicate that SOQPSK-A and –B can be detected with an suboptimum detector with a penalty of 2 dB of more as compared to OQPSK. However, the detection performance of SOQPSK can be significantly improved with a trellis demodulator using the Viterbi algorithm. The performance and implementation of this enhanced detector is the focus of this work.

Modulation Type	ρ	B	T1	T2
SOQPSK-A	1.0	1.35	1.4	0.6
SOQPSK-B	0.5	1.45	2.8	1.2

Table 1. SOQPSK-A, -B Parameters

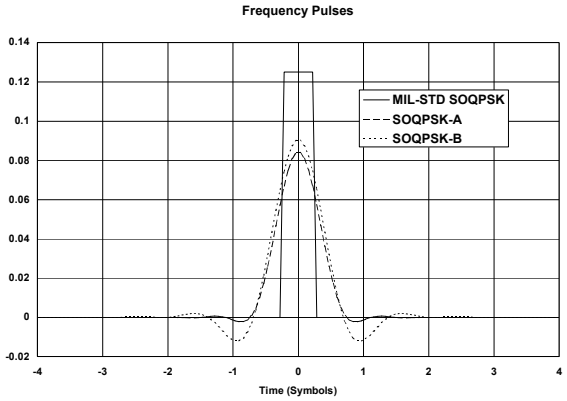

Figure 2. SOQPSK Frequency Pulse Shapes

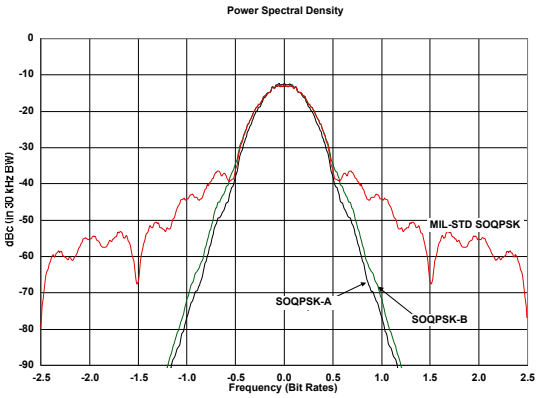

Figure 3. PSD of SOQPSK

DETECTION PERFORMANCE ANALYSIS

In order to determine the performance of the detector, the trellis description of SOQPSK will be analyzed. A bound on the probability of error can be calculated by determining the probability that the receiver will choose a particular path through the trellis (β) instead of the path that was actually transmitted (α). Of particular interest is the pair of paths (α, β) that are closest in Euclidean distance and result in one or more bit errors. The distance between these two paths is called the 'minimum distance' and is denoted by d^2_{min}. As the signal-to-noise ratio (SNR) becomes large, the error contribution caused by this 'minimum distance' event will dominate the bit error probability.

A trellis representation for the MIL-STD-188-182 version of SOQPSK is illustrated in Figure 4 and shows the constellation diagram along with the data and frequency pulses that produced the highlighted trajectory. The data to frequency mapping function has been described by Simon [3] as

$$\alpha(i) = (-1)^{i+1} d(i-1)\left(\frac{d(i) - d(i-2)}{2}\right)$$ where d(i) = 2a(i) – 1= {+1,-1} and a(i) = {0,1}

Note that α(i) only depends on the data values d(i), d(i-1), and d(i-2). This observation will be used later when a trellis notation is adopted for implementation.

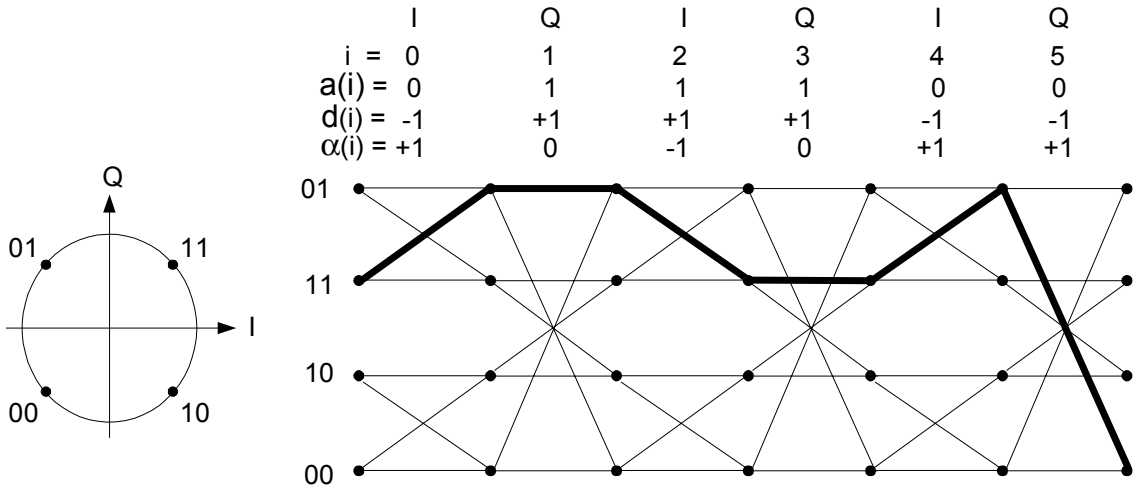

Figure 4. SOQPSK Trellis for Length T/2 Rectangular Frequency Pulse

The optimum receiver uses a pulse shape $g_R(t)$ that matches the transmitted pulse shape $g_T(t)$. Its performance can be bounded using the Euclidean distance between the paths (α, β) that are most likely to be confused at the receiver. Since they both use the same pulse shape, the distance only depends on the difference sequence γ which is defined as $\gamma = \alpha - \beta$. From [4], it is shown that the minimum distance can be expressed as

$$d^2_{\min} = \min_{\substack{\alpha,\beta \\ \alpha_o \neq \beta_o}} \left\{ \frac{1}{2E_b} \int_0^{NT} [s(t,\alpha) - s(t,\beta)]^2 dt \right\} = \min_{\substack{\gamma \\ \gamma_o \neq 0}} \left\{ \frac{2}{T} \int_0^{NT} [1 - \cos(\phi(t,\gamma))] dt \right\}$$

where $s(t,\alpha)$ is the transmitted signal, NT is the length of the observation, α and β are the sequence of frequency impulses that are different in at least the first symbol, $\phi(t,\gamma)$ is the transmitted phase and $\gamma_i = \alpha_i - \beta_i$. Figure 5 illustrates a typical error event in which the receiver mistakenly chooses a path corresponding to β instead of the actual transmitted path α. Note that before the paths split the phase difference and the accumulated distance is zero and while the paths are different, the non-negative Euclidean distance continues to increase. Once the paths remerge, the phase difference returns to zero and the accumulated distance will remain constant. Sequences pairs that are likely to have a small distance have the property that $\gamma(i)$ returns to zero (modulo 4) fairly quickly after the initial split. In order to find the difference sequence ($\gamma_{\min}$) that corresponds to a minimum distance event, one needs to first identify the valid difference sequences and compute their integrated Euclidean distance.

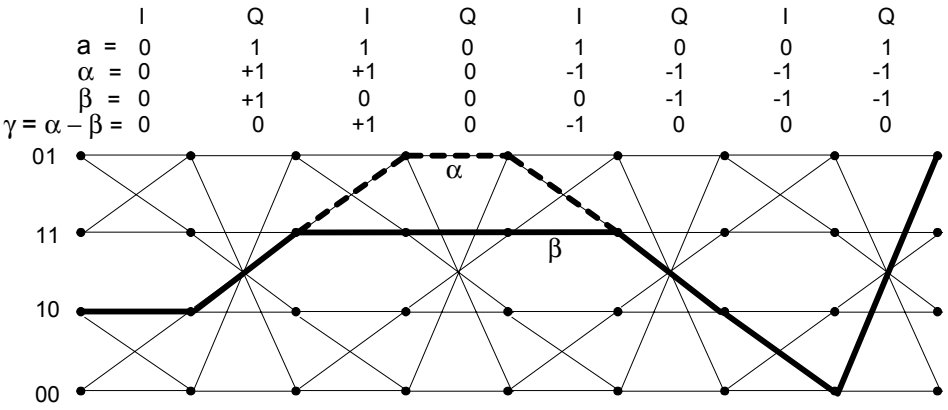

Figure 5. Example of an Error Event

For SOQPSK, the difference sequence (γ) is constrained by the function that maps data to frequency pulses. For example, $\gamma(1)$ cannot immediately return to zero after the first non-zero value $\gamma(0)$ and also $|\gamma(i) - \gamma(i-1)| \leq 2$ for all i. A phase difference tree representing valid γ that are +1 for the first value is shown in Figure 6. Note that one could choose to evaluate the set of γ's that are –1 for the first value, but they are merely the mirror images of the positive set and have the same distance values. Therefore, due to symmetry, it is only necessary to evaluate a subset of all possible γ's.

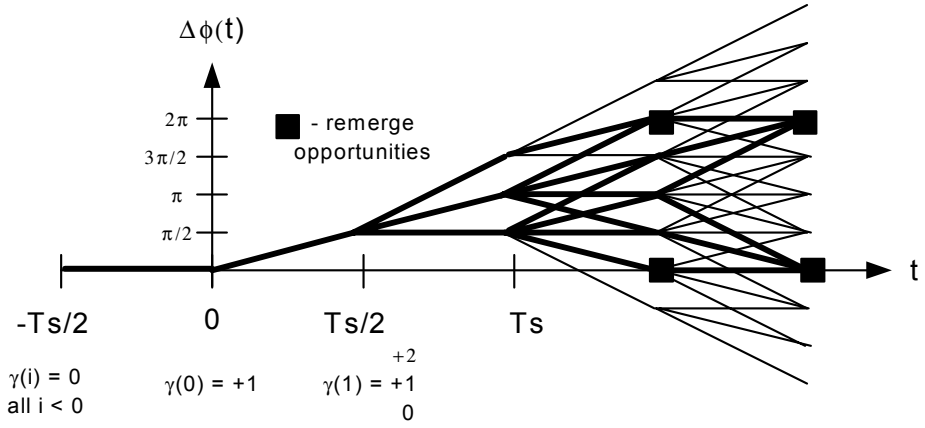

Figure 6. Phase Difference Tree

In order to identify γ_{min}, a computer program was constructed using a modified version of the "Limited Sequential Tree Search" algorithm described in Appendix A of [4]. Modifications included changing the computation period from T to T/2, using ternary-values {-1,0,+1} instead of binary inputs for α and β, and constraining the difference sequence based upon the data to frequency impulse mapping function. The distance over the interval from iT/2 to (i+1)T/2 is calculated from a finite span of the $\gamma(i)$'s, accumulated, i is incremented, and the procedure is repeated. Candidates that exceed a specified distance can be eliminated, thereby keeping the number of candidates being evaluated manageable.

The computer search determined that the γ sequence corresponding to the minimum distance error event is $\gamma_{min} = [+1\ 0\ -1]$ for both SOQPSK variants with minimum distances (d^2_{min}) of 1.5067 and 1.7412 for SOQPSK-A and –B respectively. Since this 'minimum distance' event dominates the probability of error at large SNR, the detector performance can be upper bounded by $Pe \le Q((d^2_{min}E_b/N_o)^{1/2})$.

However, a more accurate expression for the bit error probability of SOQPSK can be formulated by closely examining the trellis error events. Starting at a point where the transmit path and the path selected by the receiver diverge, there are four difference sequences of frequency pulses (γ) that are most likely to be taken as the paths remerge. Although there are many ways for the pairs to remerge, half of them can use minimum distance paths (i.e. $\gamma_{min} = [+1\ 0\ -1]$ or $[-1\ 0\ +1]$). The easiest way for the other half of the sequence pairs to remerge is by $\gamma = [+1\ +2\ +1]$ or $[-1\ -2\ -1]$ which have Euclidean distances of 2.68676 for SOQPSK-A and 2.38027 for SOQPSK-B. All of the above-mentioned paths only produce one bit error. Therefore, if the input bits are equally likely and all error events always remerge over paths that are closest in Euclidean distance, a lower bound on the probability of bit error for SOQPSK-A and –B can be expressed as

$$Pe_{SOQPSK-A} \ge \frac{1}{2}Q\left(\sqrt{\frac{1.5067E_b}{N_o}}\right) + \frac{1}{2}Q\left(\sqrt{\frac{2.68676E_b}{N_o}}\right)$$

$$Pe_{SOQPSK-B} \ge \frac{1}{2}Q\left(\sqrt{\frac{1.7412E_b}{N_o}}\right) + \frac{1}{2}Q\left(\sqrt{\frac{2.38027E_b}{N_o}}\right)$$

It is interesting to note that the same analysis applies to OQPSK with the exception that the distance for all of the γ's equal 2. Setting the distances equal to 2 in the above equation yields $0.5Q((2E_b/N_o)^{1/2}) + 0.5Q((2E_b/N_o)^{1/2}) = Q((2E_b/N_o)^{1/2})$ which is known to be the exact bit error probability for OQPSK. The lower bounds for SOQPSK turn out to be extremely tight as will be shown in a later section.

A plot of the error rate performance bounds for SOQPSK-A and -B is shown in Figure 7 along with results for similar waveforms including OQPSK and the upper bound for Feher patented FQPSK which has been shown to have a minimum distance of 1.56 [5]. Using the upper bound ($Pe \le Q((d^2_{min}E_b/N_o)^{1/2})$, the asymptotic loss relative to OQPSK is 0.6 dB for SOQPSK-B, 1.07 dB for FQPSK, and 1.23 dB for SOQPSK-A. The lower bounds for SOQPSK-A and –B are within 0.25 dB of the upper bound at a BEP of 10^{-6}. The asymptotic performance of SOQPSK-B is 0.47 dB better than FQPSK and 0.63 dB better than SOQPSK-A.

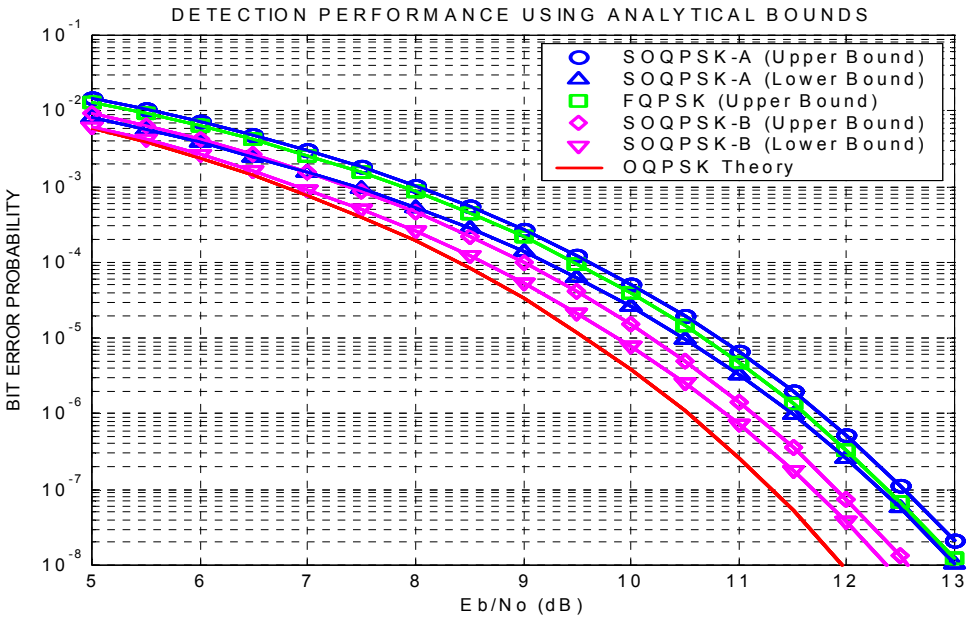

Figure 7. Detection Performance based on Euclidean Distance Bounds

TRELLIS DEMODULATOR IMPLEMENTATION

Now that analytical bounds for the error performance have been developed, the next step is to address the implementation of the trellis demodulator. Since the Viterbi algorithm will be used to recover the data, the implementation complexity will be proportional to the number of states which is determined by the length of the receive frequency pulse. In order to achieve an efficient, high-speed hardware architecture, it is desirable to process the signal at the symbol rate. A suitable state representation is suggested by observing that the transmitted signal, over a symbol interval, can be completely described by a finite span of frequency pulses and a starting phase angle. Since the frequency pulses and starting phase are a function of the source bits, the trellis state can be constructed from a fixed span of input bits. As an example, Figure 8 illustrates the notation for a trellis using a receive pulse length of $L_R = 1$ for which there are eight states of the form [a(i-1) a(i-2) a(i-3)]. The current state combined with the input data for the next symbol [a(i+1) a(i)] are sufficient to construct the received signal set required by the demodulator. The trellis diagram for SOQPSK with $L_R = 1$ is shown in Figure 9.

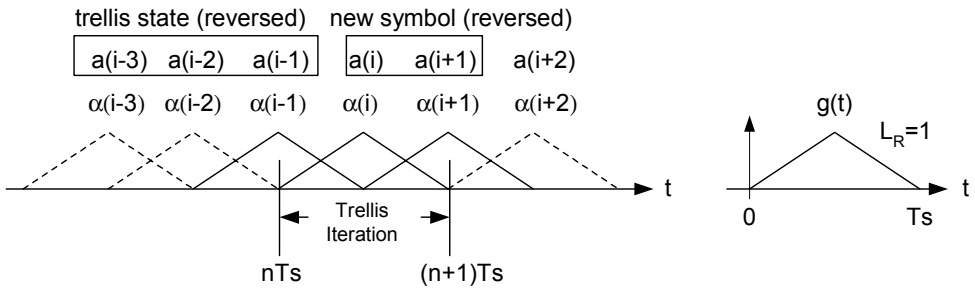

Figure 8. Illustration of Trellis Notation

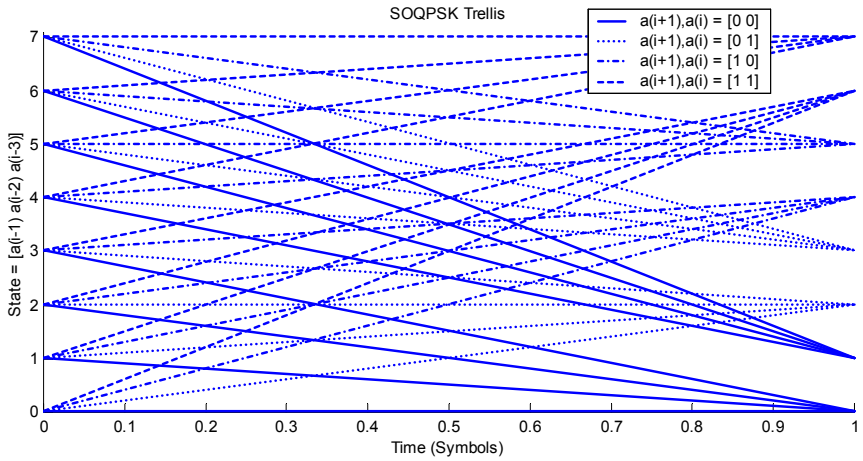

Figure 9. Trellis Connections for Frequency Pulse Length (L_R) = 1

In general, there are $2^{(2L_R+1)}$ trellis states which means that the optimum detector would require 512 and 131072 states for SOQPSK-A and –B since they extend over 4 and 8 symbols respectively. Fortunately, it will be shown that a sub-optimum version of the detectors using shortened pulses suffers virtually no penalty in detection efficiency relative to the optimum detector. Although simple truncation is not optimum, it is easy to see that if the ideal 4-symbol frequency pulse for SOQPSK-A is truncated to 2 symbols (with impulses added to account for leftover phase), it still closely matches the transmit pulse. Figures 9 and 10 illustrate this fact by plotting frequency pulses and phase trees for SOQPSK-A using an ideal pulse (L_T=4) and a truncated pulse (L_R=2) and Figures 11 and 12 compare an ideal (L_T= 8) pulse with a truncated pulse (L_R=2) for SOQPSK-B.

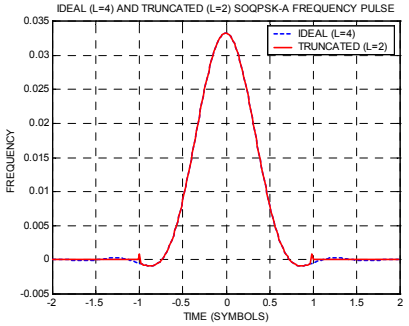

Figure 9. Pulses for SOQPSK-A

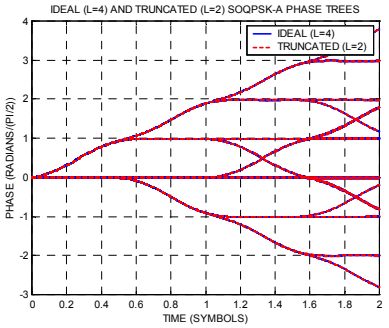

Figure 10. Phase Trees for SOQPSK-A

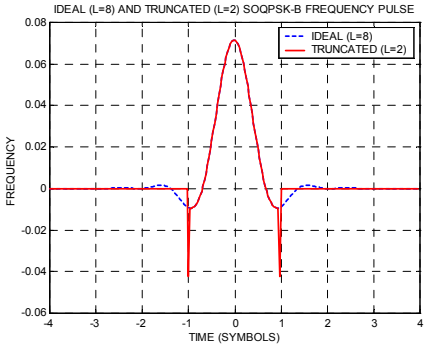

Figure 11. Pulses for SOQPSK-B

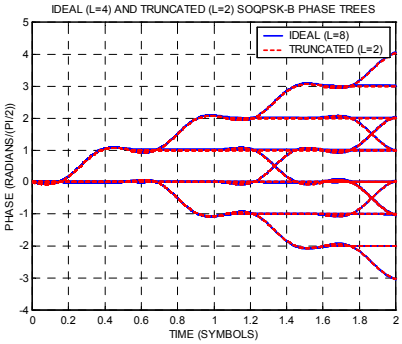

Figure 12. Phase Trees for SOQPSK-B

SIMULATION RESULTS

Simulations were performed for SOQPSK-A and –B and the results are presented in Figure 13. For comparison purposes, published simulation data for FQPSK-B using its optimum Viterbi detector [6] is also included. The simulations are for a frequency pulse truncated to one symbol time (8 state trellis) for SOQPSK-A and a two symbol length pulse (32 states) for SOQPSK-B. As expected, SOQPSK-B outperformed both optimum Viterbi detected FQPSK-B [6] and SOQPSK-A. The simulation results agree extremely well with the analytical bounds. The results, relative to OQPSK, are listed in Table 2.

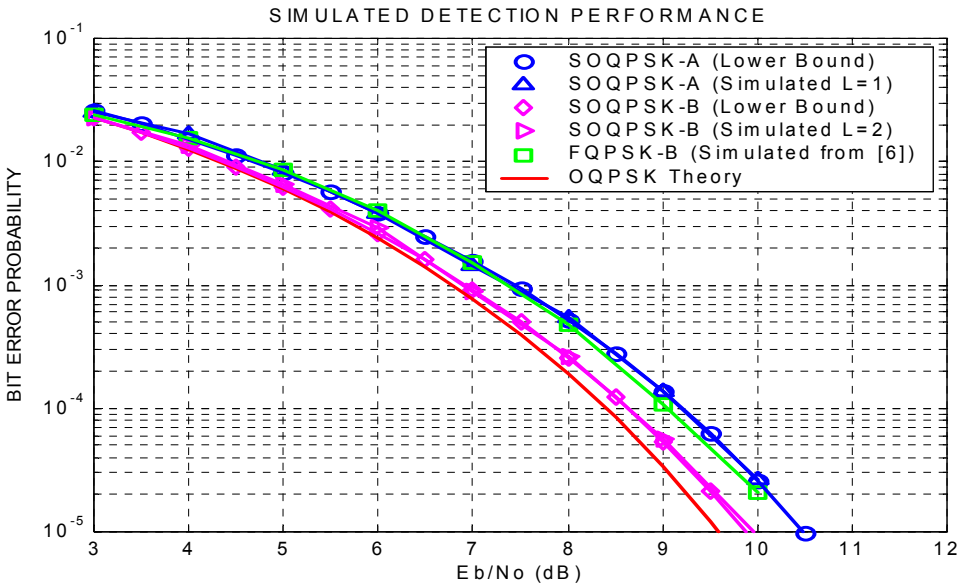

Figure 13. Simulated Results for SOQPSK

Modulation Type	Eb/No for 10^{-5} BEP (dB)	Loss Compared to Ideal OQPSK at 10^{-5} BEP (dB)
OQPSK	9.6	0
SOQPSK-A (L_R=1, 8 States)	10.5	0.9
FQPSK-B (Optimum Viterbi) [6]	10.4	0.8
SOQPSK-B (L_R=2, 32 States)	9.9	0.3

Table 2. Simulation Results

The lower bounds for SOQPSK-A and –B matched the computer simulation results extremely well over the entire range of SNR's tested. This is important since the analytical error expression can now be used with confidence for lower error rates than are practical to characterize with Monte Carlo simulations. Furthermore, it was seen that significant shortening of the transmit frequency pulse was not only feasible, but caused no discernable degradation when compared to the lower bound. This translates into a significant reduction in receiver complexity, making high-speed implementations practical.

CONCLUSIONS

A trellis detector using the Viterbi algorithm for demodulating SOQPSK-A and –B was analyzed, and upper and lower performance bounds were computed. A notation for constructing the trellis demodulator was introduced and a scheme for using shortened frequency pulse lengths to trade off performance versus hardware complexity was proposed. It was found that the sub-optimum, reduced complexity designs performed extremely well and are practical for implementation. SOQPSK-B was shown to require only 0.3 dB more power than OQPSK to achieve a BEP of 10^{-5} while FQPSK-B and SOQPSK-A needed an increase of 0.8 and 0.9 dB, respectively. These results were consistent using both analytical data and results from computer simulations.

The lower bounds for SOQPSK-A and –B are very simple expressions that provide results virtually identical to those produced through computer simulations. They will prove to be an extremely powerful and useful analytical tool for further research into this family of waveforms. Although only SOQPSK-A and –B were examined, the analysis methods and implementation concepts are applicable to any of Hill's SOQPSK variants. In summary, SOQPSK is family of non-proprietary, constant envelope waveforms that have outstanding detection efficiency and spectral containment and are ideally suited for a variety of commercial and military applications.

REFERENCES

[1] T. Hill, "An Enhanced, Constant Envelope, Interoperable Shaped Offset QPSK (SOQPSK) Waveform for Improved Spectral Efficiency", Proceedings of the International Telemetering Conference, San Diego, CA, October 2000.

[2] B. Younes; J. Brase; C. Patel; J. Wesdock, "An Assessment of Shaped Offset QPSK for Use in NASA Space Network and Ground Network Systems", Meetings of Consultative Committee for Space Data Systems", Toulouse, France, October 2000.

[3] M. K. Simon, "Bandwidth Efficient Digital Modulation with Application to Deep Space Communications," to be published as part of the JPL Deep Space Communications and Navigation (DESCANSO) Monograph Series, 2001.

[4] J.B. Anderson, T. Aulin, C.E. Sundberg, Digital Phase Modulation, Plenum Press, New York NY,1986.

[5] M.K. Simon; T.Y.Yan, "Performance Evaluation and Interpretation of Unfiltered Feher-Patented Quadrature-Phase-Shift-Keying (FQPSK)", JPL TMO Progress Report 42-137, May 1999.

[6] D.Lee, M. Simon, T.Y.Yan, "Enhanced Performance of FQPSK-B Receiver based on Trellis-Coded Viterbi Demodulation", Proceedings of the International Telemetering Conference, San Diego, CA, October 2000.